INDUSTRIAL COST EFFECTIVE N-PASHA SOLAR CELLS WITH >20% EFFICIENCY

I.G. Romijn¹, B. van Aken¹, J. Anker¹, P. Barton¹, A. Gutjahr¹, Y. Komatsu¹, M. Koppes¹, E. J. Kossen¹, M. Lamers¹, D.S. Saynova¹, C.J.J. Tool¹, Y. Zhang¹

P.R. Venema², A.H.G. Vlooswijk², C.Schmitt³, H. Kuehnlein³, N. Bay³, M. König⁴, A. F. Stassen⁴

¹ECN Solar Energy, P.O. Box 1, NL-1755 ZG Petten, the Netherlands

Phone: +31 224 56 4309; Fax: +31 224 56 8214; E-mail: romijn@ecn.nl

²Tempress Systems BV, Radeweg 31, 8171 MD Vaassen, The Netherlands

³RENA GmbH, Hans-Bunte-Strasse 19, D-79108, Freiburg im Breisgau, Germany

⁴Heraeus Precious Metals GmbH & Co. KG, Heraeusstrasse 12–14, D-63450, Hanau, Germany

ABSTRACT: The n-Pasha cell is a bifacial solar cell concept with average efficiencies between 19.8% and 20% and is optimized to enable high efficiencies with narrow distribution on wafers from the complete n-type ingots (2 to 10 Ω -cm). This reduces the yield losses from a wafer point of view, which is important since the wafer costs make up the largest part (~40%) of the total module costs for n-Pasha modules. The module fabrication itself adds up to ~35% of the module costs/Wp costs, which leaves ~25% of the costs/Wp for the cell production. We found that the costs/Wp for the 20% n-Pasha cell and module process are very similar to those of a 19% p-type cell, assuming similar wafer and module manufacturing costs. In the paper the successful implementation of a reduction of >60% in BBr₃ consumption, and a reduction of >50% in Ag consumption are described, while keeping the n-Pasha cell efficiency at the same level. According to our calculations, the achieved reduction of the Ag and BBr₃ consumption will lower the costs/Wp for n-Pasha modules below that of p-type.

The majority of the efficiency losses in the n-Pasha cell are due to recombination in the diffused layers and below the contact regions. By tuning both the emitter and BSF profile, an efficiency gain of 0.4% absolute has been obtained. Based on the simulations and experimental results, the path towards further optimization and efficiencies approaching 21% is shown.

Keywords: n-type, performance, boron, cost reduction

1 INTRODUCTION

Currently, majority of PV manufacturing still relies on mc-Si p-type. The fourth edition of the International Technology Roadmap for Photovoltaics [1] predicts a clear shift from p-type to n-type mono-Si within the crystalline Si market, with the share of n-type mono cells rising to over 30% in 2023. Compared to p-type material, n-type Cz material is known for its stable high carrier lifetimes because of the absence of light-induced degradation (LID) and its higher tolerance of the most common metallic impurities, such as Fe [2,3]. The highest efficiency crystalline silicon modules that are currently on the market are fabricated on n-type Cz material by the companies Sunpower, Panasonic and Yingli Solar [4-6].

To realize high efficiencies at low cost, ECN has developed the n-Pasha solar cell concept on n-type Czochralski (Cz) base material [7]. The n-Pasha cell is a bifacial solar cell concept with average efficiencies between 19.8% and 20%; on high quality material a top efficiency of 20.2% has been demonstrated [8].

To remain competitive in the solar market, modules with n-type cells need to be processed at low ϵ /Wp. This can be achieved by improving the cell efficiency and preferably together with reducing the cell productions costs simultaneously. The work presented in this paper demonstrates how to reduce the cost of major processing steps in the n-Pasha solar cell production process such as boron diffusion and metallization while increasing the efficiency to values above 20%.

2 N-PASHA CELL CONCEPT

2.1 Cell structure

At ECN, the n-Pasha cells are fabricated on 6 inch ntype Cz wafers. All processing steps used for the n-Pasha cell are compatible with an industrial scale. The first processing step is to texture the wafers with random pyramids using alkaline etching. The boron emitter and phosphorous BSF are formed with a co-diffusion step using an industrial tube furnace from Tempress. A 60 Ω /sq emitter is made using BBr3 as precursor. The BSF is made using POC13 as precursor and provides additional lateral conductivity at the rear side. This results in a good fill factor despite the open rear side metallization, even for cells processed on high resistivity base material (~10 Ωcm). In this way the BSF is an important element of the cell design providing a solution for reduced performance sensitivity towards variations in the n-type wafer resistivity, as will be discussed in Paragraph 2.2. Both the front and rear side are coated with SiN_x layers for passivating and anti-reflective purposes. The metal grids are printed, and the contacts on emitter and BSF are formed during a single co-firing step. Both front and rear metallization can be directly soldered so no additional metallization step is necessary to enable interconnection into a module. The module manufacturing and costs are therefore the same as for standard p-type cells.

The symmetric structure of the open front and rear side metallization ensures that the bowing of the cells will be strongly reduced when (very) thin wafers are used, which is a distinct advantage to the bowing that occurs for full area aluminum BSFs on p-type solar cells. Furthermore, the dielectric coating on the rear side results in an improved surface passivation as compared to the conventional full area aluminum rear side of p-type cells,

while the optical properties of the dielectric layer can be tuned to enable optimal (anti) reflective properties.

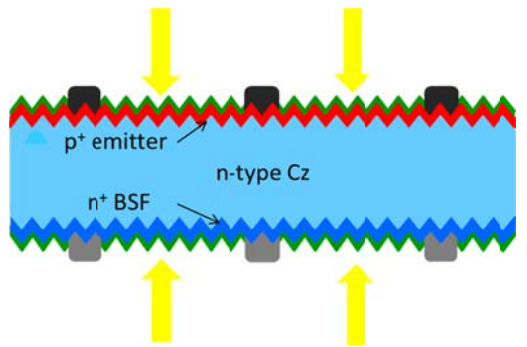


Figure 1: Cross section of the ECN n-Pasha cell. Yingli's PANDA cells are also based on this structure. It features an n-type Cz Si wafer with a boron-p+ emitter and phosphorous-n+BSF

If the cells are put in a standard mono-facial module, the refractive indices can be tuned to obtain maximum reflection in combination with the module back-sheet foil. On the other hand, the open rear side H-patterned metallization makes the n-Pasha concept very suitable for bifacial cell & module technology. This way, an even higher module output power and an increased annual energy yield can be obtained when they are placed in an appropriate way in the field. Recent results have shown that the output power of bifacial n-Pasha modules can be increased by almost 20% if the bifacial modules were placed in front of a higher reflective background [9].

2.2 Material dependence

Due to the higher segregation coefficient of phosphorous compared to boron, the resistivity distribution in P-doped, n-type Czochralski (Cz) grown ingots is typically 2 to 3 orders larger than that in B-doped, p-type Cz ingots. The n-Pasha cell process is optimized to enable high efficiencies with narrow distribution on wafers from the complete n-type ingots, with a distribution from 2 to 10 Ω -cm. This optimization involves both the doping of the diffused areas and the metallization pattern on front and rear side. The results for V_{oc} , I_{sc} , FF and efficiency are shown in Figure 2 as a function of base resistivity.

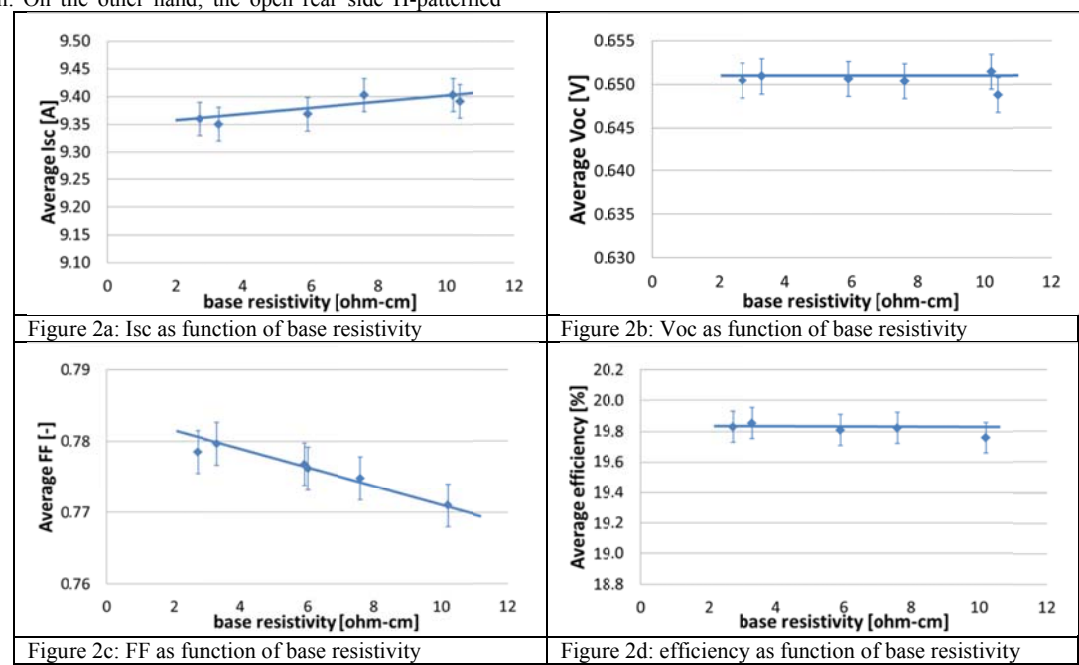


Figure 2: IV characteristics of n-Pasha cells as a function of base resistivity

The values shown in the graphs are averaged values over several experimental 'baseline' runs. In each baseline run 24 wafers originating from 5 different parts -with different base resistivity- of the ingot are processed. The value for I_{sc} increases with higher base resistivity (and thus with lower base doping) because of less recombination losses. The value for V_{oc} remains stable, as the V_{oc} is determined by both the recombination losses and the base doping which compensate each other at lower base doping. The FF decreases at higher base resistivity, naturally due to higher resistive losses. The decrease in FF is compensated by the increase in I_{sc} , resulting in a stable, high efficiency of 19.8%.

Using the n-Pasha cell concept, on specially selected, high quality material average efficiencies of 20% (10

cells) and a top efficiency of 20.2% have been achieved [8].

3 COST REDUCTION

To remain competitive in the solar cell market, solar cells need to be processed at lower costs. This can be achieved by improving the efficiency and reducing the production costs at the same time. In this Paragraph (3), the reduction of production costs will be discussed, while efficiency improvements will be described in the next Paragraph (4).

3.1 Cost built up

The n-Pasha module costs/watt-peak are built up from three parts: 1) wafer fabrication (39%), 2) cell production (26%) and 3) module production (35%).

While at the moment the costs for n-type Cz wafers may be higher than that for p-type Cz, in principle there is no fundamental reason why the costs of n-type should be higher than for p-type. Furthermore, since with the n-Pasha cell concept the complete ingot can be used to process high efficiency solar cells, the yield losses will be small.

The module manufacturing cost of n-Pasha modules are comparable to those of p-type ones, as the same interconnection and encapsulation technology can be applied. The cell production costs for n-Pasha cells can be split into the different processing steps, as is shown in Figure 3.

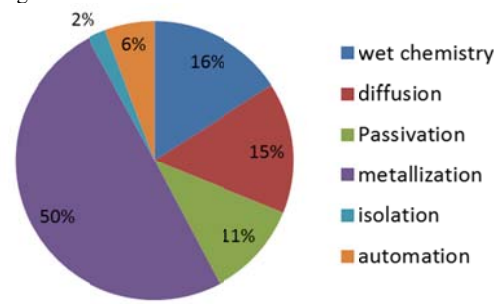


Figure 3: Relative contribution to n-Pasha cell costs of specific processing steps

The processing steps that contribute most to the costs are metallization, wet chemistry and diffusion. Different measures that are taken to reduce these costs are evaluated in the following paragraphs.

3.2 BBr₃ reduction

An infinite boron doping source is of importance to have a good control and reproducibility of the doping profile: If the dopant source is infinite, the profile is only determined by the diffusion temperature and time. For economic reasons, it is of importance to create an infinite source with a minimum amount of doping precursor. A well-established standard process for the n-Pasha cell [10] and the use of doping profile monitoring by ECV has allowed to optimize the gas flows in the BBr₃ process and at the same time monitor the doping profiles and cell output. In this way a reduction of more than 60% in BBr₃ consumption per wafer has been achieved without compromising to the process throughput and cell output. Table I shows cell results with this process on a lab scale with 24 wafers. Small differences are observed which are within standard deviations and on a production scale so far no significant differences in cell performance have been observed. The process has already been successfully implemented in industrial n-Pasha cell lines.

Table I: Average cell IV characteristics for n-Pasha cells with different BBr₃ processes

BBr3 process	I _{sc} [A]	$egin{array}{c} \mathbf{V_{oc}} \ [\mathbf{V}] \end{array}$	FF [%]	Eta [%]
original	9.36	0.651	78.0	19.87
Reduced consumption	9.39	0.649	77.8	19.82

3.3 Ag reduction

Reducing the Ag consumption has been a driving force to improve the cost effectiveness of the n-Pasha solar cells as well. In preceding years, large efforts have been taken to reduce the silver consumption both on the front and on the rear side of the n-Pasha cells [9]. In combination with the improvements in efficiency, this contributed to a substantial reduction in mg Ag per Watt-peak [8]. In 2013, this work has continued. Application of improved low Ag containing pastes on the one hand, and further optimization of the metallization patterns on the other hand have enabled further reductions in Ag consumption. The reduction in silver consumption per watt-peak from 2011 to 2013, for each year at the time of this conference, is shown in Figure 4. The silver consumption in 2013 is less than 50% to that of 2011. The 2013 n-Pasha cell has an average efficiency of 20%, while that of 2011 was 19%. As a reference case, the Ag consumption of a 19% p-type cell is shown. To make a fair comparison, the costs of the aluminum consumption for the p-type cells have been recalculated in terms of the equivalent milligrams of silver for the rear side, since the aluminum is absent in the case of n-pasha cells.

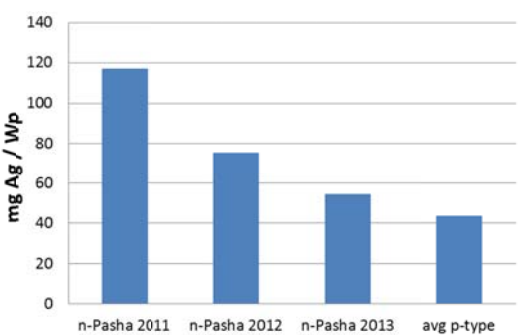


Figure 4: Reduction in silver consumption per watt-peak from 2011 to 2013, for each year at the time of this conference. The 2013 n-Pasha cell has an average efficiency of 20%. As a reference case, the Ag consumption of a 19% p-type cell is shown

3.4 n-Pasha costs vs p-type

The total costs per watt-peak for a 20% n-Pasha and a 19% p-type cell have been calculated. For the p-type cell, the 19% efficiency is assumed to be the stabilized efficiency, thus *after* LID. Assuming the same wafer and module costs, the costs/Wp for the n-Pasha case were in 2012 slightly above that of the p-type reference due to the higher metallization and diffusion costs. However, after implementing the reductions described in Paragraph 3.2 and 3.3, the total costs for n-Pasha have decreased. Due to the higher efficiency, resulting in a higher Watt-peak output, we found that costs in €/Wp for n-Pasha are now even slightly below that of a 19% p-type reference. All three scenarios are summarized, relative to the p-type reference, in Figure 5.

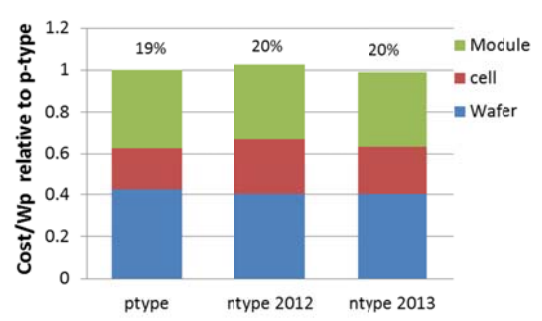


Figure 5: Cost/Wp for two n-Pasha scenarios, relative to a 19% (stabilized efficiency after LID) p-type reference

4 EFFICIENCY IMPROVEMENTS

To determine the most effective route towards further efficiency improvement of the n-Pasha cell, an extensive loss analysis based on experimental results as well as 2-dimensional modeling of the cell has been performed and described in a different contribution to this conference [11]. According to the analysis, the major loss factor is the recombination in the cell, which stems mainly from the diffused parts of the cell and the emitter contacts, and adds up to a loss of ~4% absolute in efficiency. Efficiency improvements can be realized firstly by modifying the emitter and BSF, secondly the recombination at the contacts needs to be reduced.

4.1 Emitter and BSF improvement

The recombination losses from the diffused layers stem mainly from Auger recombination in the emitter / BSF itself, and from the recombination at the surface of the layer. The Auger recombination in the doped layers can be reduced by decreasing the overall doping, either by reducing depth of the doping profile or by reducing the peak doping level. In general, both result in an increase in R_{sheet} .

The recombination at the surface can be reduced by using the appropriate passivating layer that provides optimal chemical and field effect passivation. A comparison of different passivating layers and their capability to passivate n-type emitters and BSFs is described in another contribution to this conference [12]. In this study, the surface passivation layers were kept the same.

In Figure 6, the Implied $V_{\rm oc}$ is shown for four different emitter profiles, with decreasing depth and increasing $R_{\rm sheet}$.

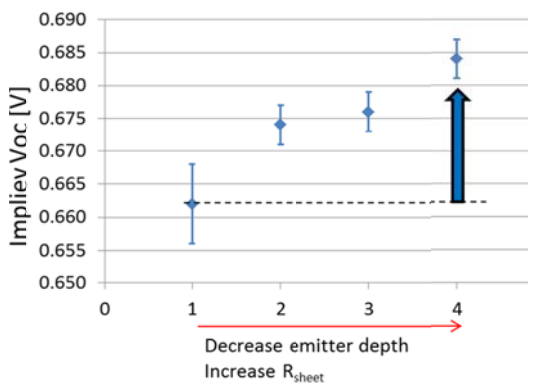


Figure 6: Increase in Implied Voc for different emitter profiles with reducing depth (more shallow) and increasing R_{sheet}

The first value of 662 mV (for profile 1) corresponds to our standard 60 ohm/sq emitter with an emitter recombination current $J_0 \sim 100~\text{fA/cm}^2.$ For the 4^{th} emitter profile, with an increased $R_{\text{sheet}} \sim 120~\text{ohm/sq}$, the Implied V_{oc} is >20~mV higher, reaching values around 685 mV, corresponding to $J_0 < 50~\text{fA/cm}^2.$ The gain in V_{oc} would correspond to an increase in efficiency of $\sim 0.7\%$ absolute.

Thus, for well passivated surfaces, J_0 indeed decreases for decreasing emitter doping resulting in a substantial gain for V_{oc} . However for areas that are not (well) passivated, such as below the contacts, J_0 depends on the shielding of the emitter [11]. Reducing the emitter doping will therefore lead to an *increase in* J_0 . If homogeneous emitters are used, both effects counteract each other and need to be well balanced to obtain an increase in efficiency. Best cell results were obtained for emitter profile 2, with an efficiency gain of 0.2% absolute, from 19.7 to 19.9%.

Naturally, when the emitter is improved, the recombination in the BSF will become more limiting. Similar principles as described above for the emitter also apply to the BSF; after improving the emitter profile as a next step the BSF profile has been further tuned towards lower doping as well. This yielded an additional efficiency gain of 0.2% absolute, towards 20.1% (I_{sc} : 9.39 A; V_{oc} : 0.654 V; FF: 78.1%). The results of both experiments are summarized in Figure 7.

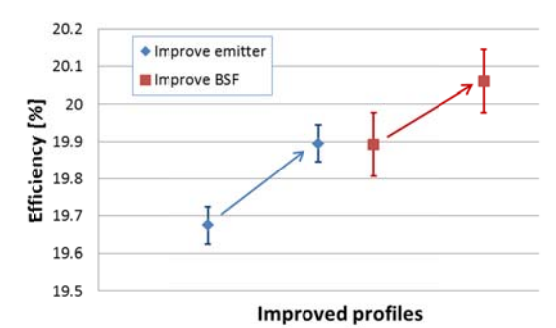


Figure 7: Increase in efficiency for improved emitter and subsequently improved BSF profiles

4.2 Outlook towards 21%

In order to achieve even higher efficiencies, both emitter and BSF profiles have to be improved further towards less Auger recombination. So far, a gain of 0.4%

has been achieved. Based on Implied V_{oc} measurements, the potential gain in efficiency for the combined optimization of emitter and BSF is around 0.7% absolute. To obtain even higher efficiencies, the emitter contact recombination needs to be further reduced as this will counter the emitter improvements should the profiles become too shallow. One way to achieve this, is to use a selective emitter approach. In this way, emitter profiles for contact and non-contact regions can be tuned separately. Another method to reduce the contact recombination is by improving the contact mechanism itself; for instance by so called 'passivated' contacts or by using less aggressive metallization pastes. Both approaches are currently being evaluated at ECN, on both an efficiency and cost level.

Besides reducing the recombination, also other parts of the n-pasha cell can still be improved. Optical losses also still play a substantial role. A significant gain in current density would be obtained by adopting a MWT design [13], while also reduction of (free carrier) absorption, improved (anti-)reflection and improved light trapping can contribute to a current gain. For the latter two, the dielectric coatings, especially at the rear, and their interaction to the (bifacial) module will be investigated.

5 SUMMARY AND CONCLUSIONS

The n-Pasha cell concept is shown to be a robust process, that enables stable and high efficiencies (19.8% average) over a wide base resistivity range. This will reduce the yield losses of n-type Cz ingots. On specially selected, high quality material, an average efficiency of 20% with top efficiency of 20.2% has been achieved.

We found that the costs/Wp for the 20% n-Pasha cell and module process are very similar to those of a 19% p-type cell, assuming similar wafer and module manufacturing costs. According to our calculations, the achieved reduction of the Ag and BBr $_3$ consumption will lower the costs/Wp for n-Pasha modules below that of p-type.

The majority of the efficiency losses in the n-Pasha cell are due to recombination in the diffused layers and below the contact regions. By tuning both the emitter and BSF profile, an efficiency gain of 0.4% absolute has been obtained. Based on the simulations and experimental results, the path towards further optimization and efficiencies approaching 21% has been shown.

The combination of efficiency improvements and the cost reduction makes the n-Pasha cell concept a very cost-effective solution for manufacturing highly efficient solar cells and modules.

6 ACKNOWLEDGEMENT

AgentschapNL is acknowledged for financial support.

7 REFERENCES

- [1] SEMI PV Group Europe 2013, International technology roadmap for photovoltaic (ITRPV): Results 2012, 4th edn. (March).
- [2] S. Glunz et al. 1998, Proc. 2nd WCPEC, Vienna, Austria, p. 1343.

- [3] D. Macdonald & L.J. Geerligs, 2008, Appl. Phys. Lett., vol 92, p. 4061
- [4] P. Cousins et al., 2010, 36th IEEE PVSC, Hawaii, USA
- [5] T. Mishima et al., 2011, Solar Energy Mater. & Solar Cells 95, p18-21
- [6] D. Song et al., 2012, Proc. 38th IEEE PVSC, Austin, USA
- [7] A.R. Burgers et al., 2011, Proc. 26th EUPVSEC, Hamburg, Germany
- [8] I.G. Romijn et al., 2013, Photovoltaics International, 20th edn, p33
- [9] I.G. Romijn et al., 2012, Proc. 27th EUPVSEC, Frankfurt, Germany
- [10]Y. Komatsu et al., 2009, Solar Energy Mater. & Solar Cells 93, p750 752
- [11]G. J. M. Janssen et al., to be published at this conference (2CV.3.20)
- [12]D. S. Saynova et al., to be published at this conference (2BV.1.46)
- [13]N. Guillevin et al., 2012, Proc 22nd PVSEC, Hangzhou, China